Journal of Structural Geology 30 (2008) 1095–1108

Contents lists available at ScienceDirect

Journal of Structural Geology

journal homepage: www.elsevier.com/locate/jsg

Structural characterization of deep-water deposits in a foreland basin, Silla Syncline (Chilean Patagonia), with applications to depositional processes

Joseph Gonzales*, Atilla Aydin

Department of Geological and Environmental Sciences, Stanford University, Stanford, CA 94305, USA

ARTICLE INFO

Article history:
Received 23 August 2007
Received in revised form 7 May 2008
Accepted 8 May 2008
Available online 15 May 2008

Keywords:
Fault network
Depositional behavior
Deep-water sediments
Magallanes foreland basin
Silla Syncline

ABSTRACT

Based on our detailed structural characterization, we examine possible relationships between thrust faults and strike-slip faults and thrust-cored folds and depositional units in the Silla Syncline, a 4 km wide fold composed of fine-grained mudstone, coarse sandstone and conglomerate deposits of the Cerro Toro Formation in the Magallanes foreland basin, Chilean Patagonia. The syncline is bounded on its western flank by an asymmetric anticline and on its eastern flank by a broad zone of thrust faults and associated folds, which are oriented sub-parallel to the syncline axis. Deposition of the coarse-grained units of the Silla Syncline appears to have taken place in this structurally defined trough controlled primarily by thrust fault related growth structures flanking the syncline.

The syncline and surrounding area have also been deformed by two sets of strike-slip faults, one right-lateral and one left-lateral. The strike-slip and thrust faulting operated contemporaneously for much of their active periods, although it appears that thrust faulting, confined within the fine-grained units, initiated slightly earlier than strike-slip faulting. In addition, younger igneous intrusions at high angle to bedding generally localize along the strike-slip faults. The cross-cutting relationships among the intrusions, strike-slip faults, and flexural slip faults show that all these structures were active during the same period, which extends beyond mid-Miocene.

These conclusions support the premise that structures in deep-water sediments are important for understanding not only the deformation of a foreland basin, but also its depositional architecture.

1. Introduction

Outcrop exposures of deep-water clastic sediments are useful analogs for modern day reservoirs and aquifers, and understanding how these sediments deform can provide information on reservoir heterogeneities. The Magallanes Basin, a foreland basin located in southern Chile (Fig. 1A), exposes deep-water clastic strata of the Andean foreland (Katz, 1963), and provides an opportunity to examine the deformation mechanisms of a foreland basin at the outcrop scale. Previously, structural aspects of the basin have been studied at a regional scale (Katz, 1962; Dalziel, 1981; Winslow, 1981; Wilson, 1991; Altenberger et al., 2003; Kraemer, 2003; see for example, Fig. 2) but detailed structural characteristics have not been documented. Additionally, the detailed behavior and patterns of different fault types, including their formations, histories, and interrelationships in a foreland basin setting in general are not well known. In this study we focus on the Silla Syncline and its surroundings. The syncline itself, a 4 km wide, open fold (Fig. 3), is primarily in coarse-grained strata of the Cerro Toro Formation and is flanked by fine-grained sandstones and mudstones. The syncline and surrounding area have undergone several types of deformation, including fracturing, folding, thrust and reverse faulting, and strike-slip faulting. Other prominent features are numerous igneous intrusions. Based on our detailed structural observations, we address possible relationships between thrust faults and strike-slip faults, thrust-cored folds and depositional units, and strike-slip faults, flexural slip faults and intrusions. We propose a conceptual model for the deformation history of the study area, including the orientation and localization of coarse-grained, deep-water channel deposits. This model offers a basis for understanding deposition and ensuing deformation of deep-water clastic strata in a foreland basin.

2. Geologic setting

The study area is centered about 51°S and 73°W, in the western Magallanes Basin, and to the east of the N–S oriented Andean

* Corresponding author. Fax: +1 650 725 0979.
E-mail address: joeg1@pangea.stanford.edu (J. Gonzales).

0191-8141/$ – see front matter © 2008 Elsevier Ltd. All rights reserved.
doi:10.1016/j.jsg.2008.05.002

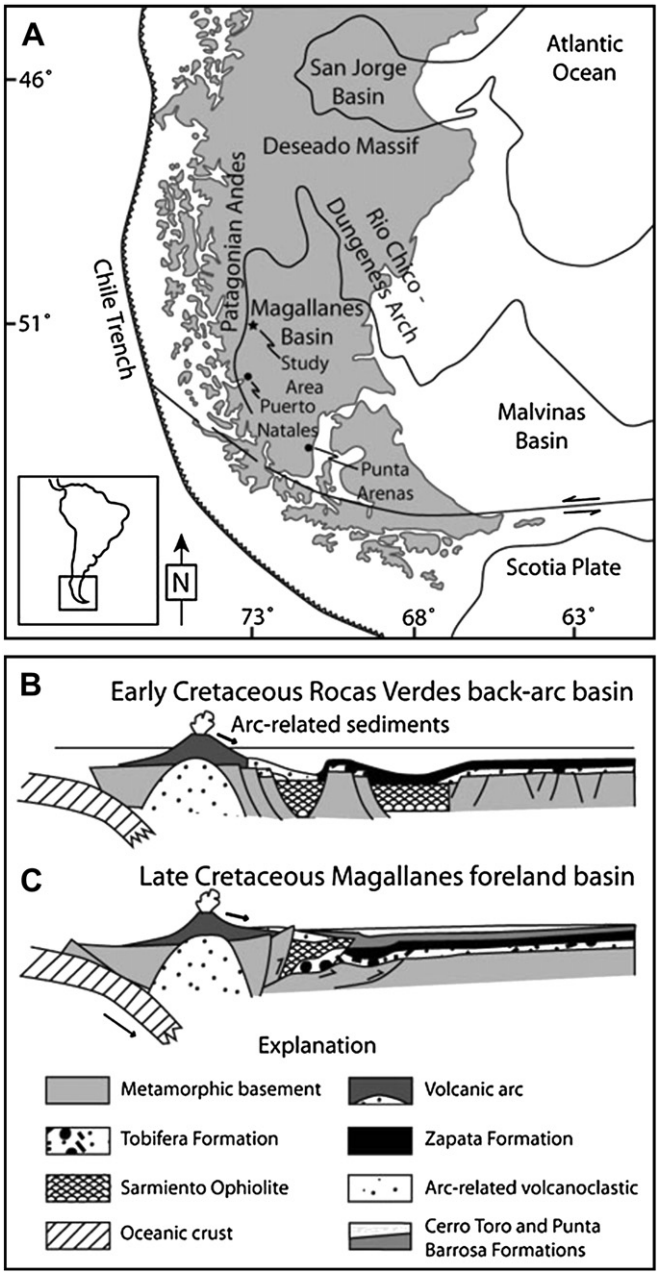

Fig. 1. (A) Location of Magallanes basin, modified from Biddle et al., 1986. (B) and (C) Basin evolution diagrams, modified from Wilson (1991) and Fildani and Hessler (2005).

orogenic belt in Chilean Patagonia, South America. It is approximately 110 km north of the town of Puerto Natales, and approximately 400 km north of the city of Punta Arenas. Geographically, the study area is located within the Parque Nacional Torres Del Paine, adjacent to Lago Nordenskjold in the north, Lago Pehoe and Lago Grey in the west, Lago Sarmiento in the east, and Lago del Toro in the south (Fig. 2). The national park owes its uniqueness to distinctive igneous intrusions, glaciers, and colorful lakes.

The Magallanes Basin has been identified as a retro-arc foreland basin (Wilson, 1983, 1991), related to the Andean Orogeny (Fig. 1B and C). Prior to the orogeny, in the Late Jurassic to the Early Cretaceous, the area had undergone extension related to the breakup of Gondwana (Bruhn et al., 1978; Gust et al., 1985; Fildani and Hessler, 2005). This extension resulted in the development of a back arc basin, which has been named the Rocas Verdes back arc basin, and ophiolitic rocks present south and west of the park are thought to be remnants of this basin (Dalziel et al., 1974; Dalziel, 1981). The change from extensional to compressive environments is believed to be the result of the eastward progression of Andean orogenic activity.

The Magallanes foreland basin was filled in the Late Cretaceous to early Tertiary, with approximately 7 km of sediments (Wilson, 1983, 1991; Biddle et al., 1986). The strata in the Silla Syncline are part of the Cerro Toro Formation (Crane, 2004), which is present throughout much of the Magallanes Basin (Fig. 2). Fig. 4 is a stratigraphic column showing the details of the sedimentary deposits for the Upper Cretaceous. Except in certain locations, the Cerro Toro Formation conformably overlies the Punta Barrosa Formation, and grades upward to the overlying Tres Pasos Formation (Katz, 1963; Fig. 2). The thickness of the Cerro Toro Formation is estimated at 2000–2500 m (Katz, 1963; Wilson, 1991). The age of the formation based on fossil evidence is middle to upper Senonian (Katz, 1963), but might be younger based on recent zircon analysis of the underlying Punta Barrosa Formation (Fildani et al., 2003). The lithology of the Cerro Toro Formation is dominantly mudstone and thin-bedded fine sandstone turbidites (Fig. 5A) containing several thick (at times greater than 200 m) sequences of conglomerate and coarse sandstone deposits (Fig. 5B) (Crane, 2004). In addition to turbidites, there is evidence for debris and slurry flows within the formation (Crane, 2004).

Sediment composition and depositional style indicate that the Cerro Toro Formation was deposited in deep water, with a paleobathymetry of approximately 2000 m (Katz, 1963; Fildani and Hessler, 2005). Crane (2004) interpreted the coarse-grained units to represent filled channel systems located in incised submarine valleys (Fig. 6).

Throughout its evolution, the general morphology of the basin is that of an approximately north–south oriented axial basin (Wilson, 1991). Paleocurrent data in the Cerro Toro as well as Punta Barrosa formations show transport directions to the south and southeast (Wilson, 1991; Crane, 2004; Fildani and Hessler, 2005). The Silla Syncline, located on the western slope of the basin, is interpreted as a feeder channel to the basin floor (Crane, 2004; Hubbard, 2006; Fig. 6). Crane (2004) also identified several members of distinct channel deposits within the syncline, indicating that depositional channels were migrating during sedimentation, although the overall transport direction, based on the paleocurrent data, remained more or less the same for all the channels.

During the mid-Tertiary, parts of the Magallanes Basin were subjected to extensive intrusive activity, which resulted in igneous dikes and sills as well as the distinctive appearance of the mountains of the Parque Nacional Torres del Paine. The intrusions are predominately mid-Miocene in age. The intrusive rocks are divided into 5 separate complexes characterized by mildly alkaline to calc-alkaline magmatism, which indicates mantle origins for the magma (Altenberger et al., 2003). The major driving force for this intrusive activity was likely the subduction of the Antarctic plate underneath the South American plate to the west of the study area (Fig. 1C).

3. Objectives

The objectives of this project are twofold: First, to use detailed structural observations to characterize the deformation of the deep-water deposits of the Silla Syncline and its surroundings. This focus is important given that these types of deposits are reservoir rocks for a great portion of the petroleum resources in the United States and Mexico. The second objective is to examine the relationships between the structural features and the location and orientation of coarse-grained deposits. Finally, we present a conceptual model of the deformational history, and show that the resulting structures were influential in a variety of processes

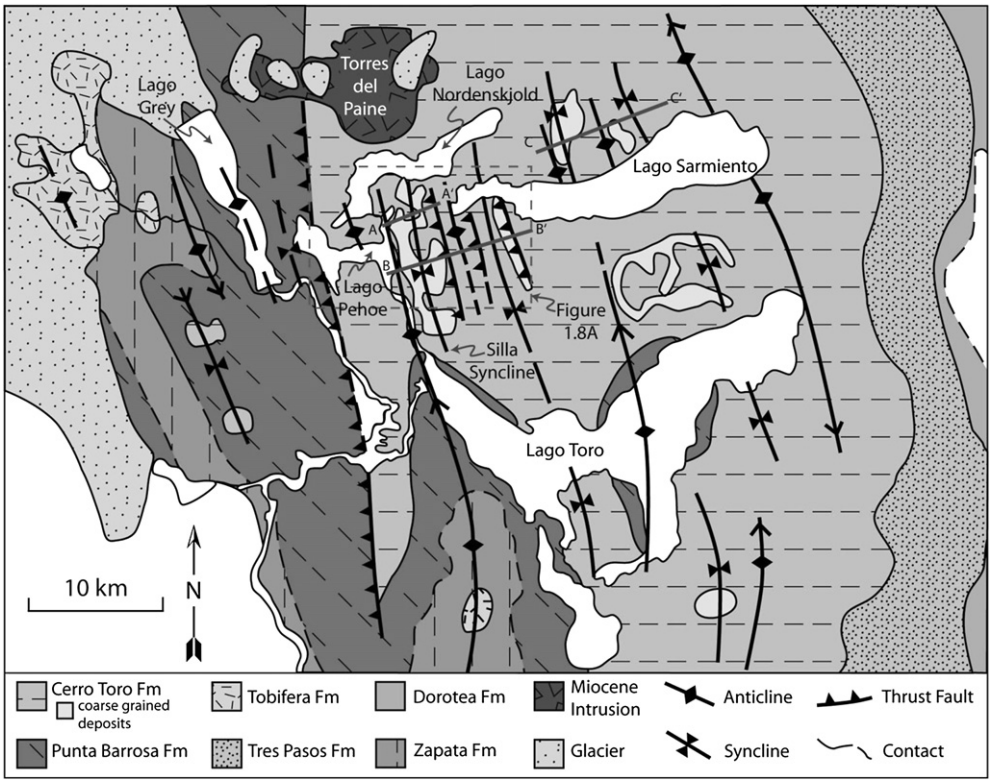

Fig. 2. Geologic map of the Silla syncline and surrounding area, modified from Wilson (1991). Cross section locations are shown and the dashed box is the location for the structural map in Fig. 7A.

including the deposition of coarse-grained sandstones and conglomerates.

4. Structural characterization

Using aerial photographs as base maps, we mapped the major structural features of the Silla Syncline and surrounding area in the field during three field sessions from 2004 to 2006. The product is a structural map (Fig. 7A) showing major folds, thrust faults, and two sets of strike-slip faults, which are each described in the following sections. We used ground photography-based mapping to establish the internal texture and geometry of the faults and their predecessor fracture systems. Also detailed are the character of the igneous dike intrusions and their spatial and temporal relationships to the faults and folds. The locations of these detailed observations are marked in Fig. 7B.

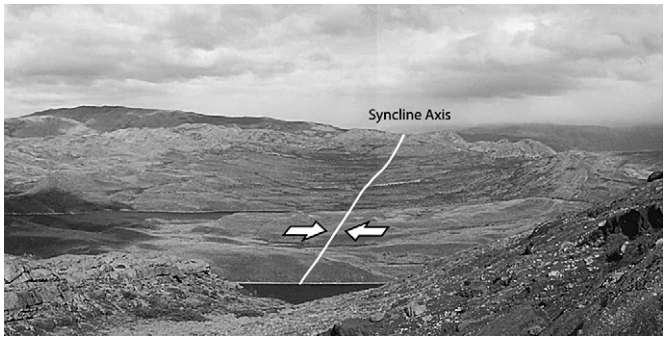

Fig. 3. View to the south along the Silla syncline. The width of the syncline is approximately 4 km.

4.1. Structural elements

4.1.1. Folds and thrust faults

There are a series of folds with north–south axial trends, originally mapped by Wilson (1983, 1991). Fold amplitude and wavelengths are interdependent with lithology. Large wavelength folds (up to 8 km) involve in the coarse-grained units with thick beds, and smaller wavelength folds occur in the fine-grained units with thin beds. The Silla Syncline is the largest of the mapped folds, with a width of up to 4 km. The syncline plunges to the north and extends to the base of the Torres del Paine intrusion. Crane (2004) identified three coarse-grained channel deposit members of the Cerro Toro Formation within the syncline (Fig. 4B). East and west of the syncline, the lithology is dominantly mudstone with isolated fine-grained sandstone layers, interpreted by Crane (2004) as turbidites. These deposits display folds with smaller wavelengths than that of the Silla Syncline (Figs. 2 and 7A). In some cases, these folds are associated with a zone of thrust faults at their cores or limbs.

One of these folds, which is significant for the structural framework of the Silla Syncline and the depositional framework of the coarse-grained units therein, marks the western boundary of the syncline following the eastern edge of Lago Pehoe (Fig. 7A). We have informally named this fold the Lago Pehoe Anticline (LPA), a relatively smaller fold with respect to the Silla Syncline, within fine sandstones and mudstones. The anticline is asymmetric, with the eastern limb dipping steeper than the western limb.

The eastern boundary of the Silla Syncline is marked by a zone of thrust faults and associated folds. This boundary structure is here informally named the Lago Sarmiento Chico Fault Zone (LSCFZ) (Fig. 7A). The LSCFZ is a complex zone of deformation, but its first order structure is a broad antiform, with bedding transitioning from west dipping on the syncline side to steeply east dipping and

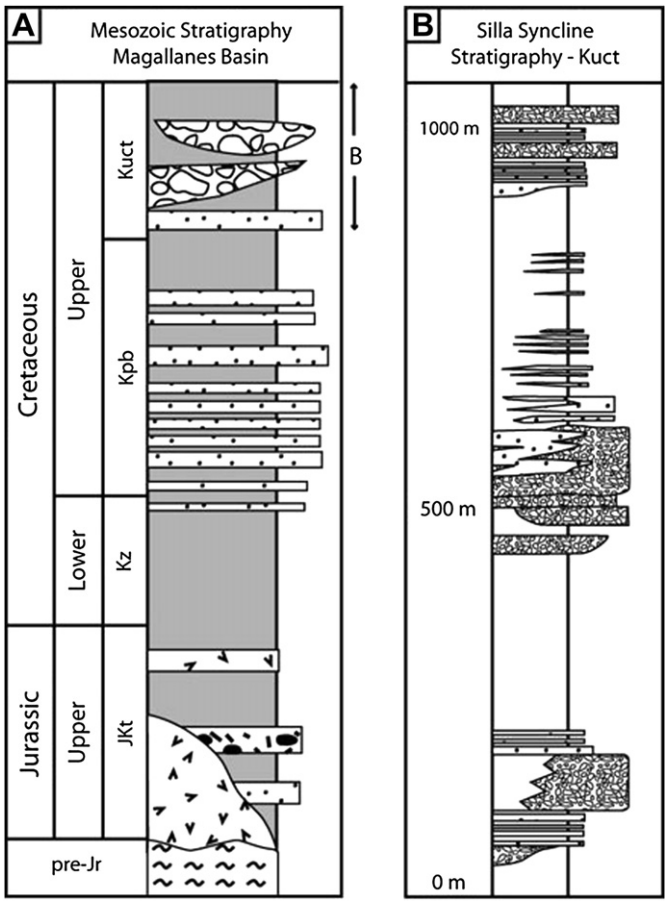

Fig. 4. (A) Stratigraphic column showing Upper Cretaceous sediments of the Magallanes basin, with a detail (B) of the Silla Syncline stratigraphy. From Crane (2004).

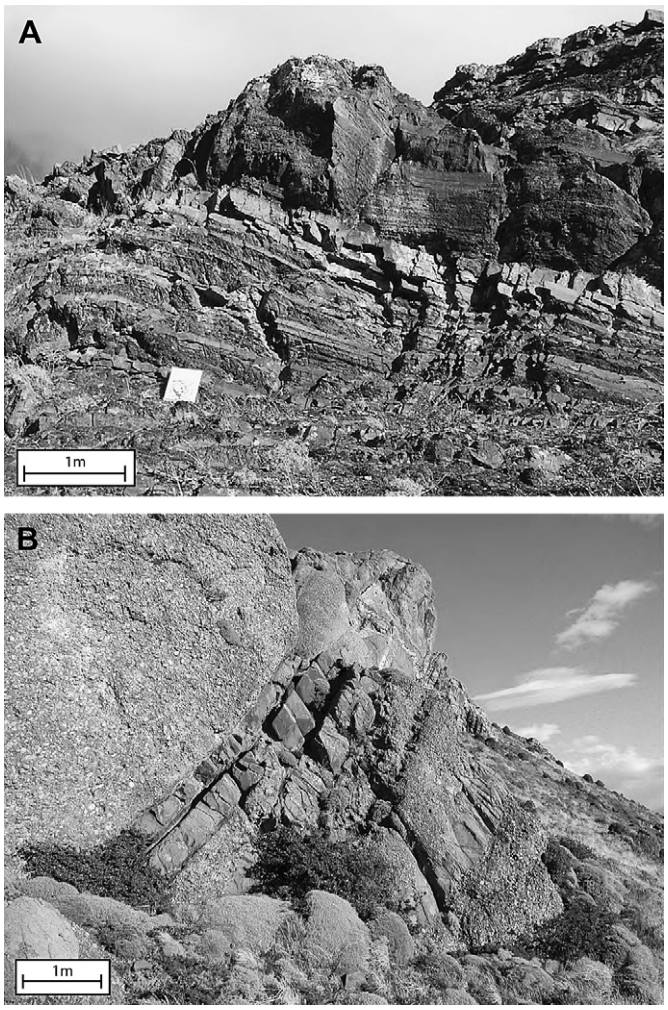

Fig. 5. (A) Typical fine-grained sediments in the study area, and (B) typical coarse sandstone and conglomerate deposits.

locally overturned on the eastern side of the zone (Fig. 8). At the core of the antiform, there are numerous thrust faults (Figs. 8, 9, and 10) and truncated rootless folds (Fig. 10A), sub-parallel to the axis of the Silla Syncline with an average orientation of 168° (angles are measured clockwise from north, also for simplicity any fault displaying reverse or thrust motion is referred to as a thrust fault). The LSCFZ also marks the change in lithology from coarse-grained within the syncline to the west to fine-grained immediately to the east. Due to this sharp lithological change from coarser to finer lithologies across the zone, it was not possible to accurately measure the total offset accommodated by the fault zone, but it is likely to be on the order of several tens of meters.

Individual thrust faults occur at different scales, with visible offsets ranging from approximately tens of centimeters to about 30 m (Figs. 8, 9, and 10), and accommodate E–W shortening, and east-directed transport. Most of the thrust faults are confined within fine-grained units and do not occur in the coarse-grained units within the Silla Syncline. Typically, the fault zones contain calcite (Fig. 9B) or other unidentified minerals, and breccia, possibly due to high fluid pressure. Thrust faults are either associated with folds displaying complicated fault geometries (Fig. 10A), or are at low-angle to unfolded bedding (Fig. 10B). These low-angle faults form wedges of rock between bedding and the faults. The wedge-forming faults generally accommodate several meters of offset and are present in somewhat stiffer fine-grained sequences, whereas fold and fault coupling occurs in alternating mudstone and fine-grained sandstone sequences. Discontinuous and rotated beds of coarser grain sizes are typically found within thrust fault zones in these alternating lithologic sequences. In addition to thrust faults, bed parallel slip occurs along layer boundaries and within finer-grained sediments. Slickenside orientations and offset layers show that slip occurred in a top to the west sense in the western limb of the Silla Syncline and top to the east sense in the eastern limb, consistent with flexural slip folding (see inset in Figs. 9B, 10B and 15).

4.1.2. Strike-slip faults

Strike-slip faults form in an apparent conjugate pattern, with a NE–SW striking right-lateral set and an E–W striking left-lateral set (Fig. 7A). These faults have geomorphic expressions in the form of deeply incised valleys (Fig. 11). However, because the valleys are heavily vegetated, there are few exposures of the fault core or fault damage zone. Katz (1962) identified some of these valleys and their associated right-lateral faults, but he was not aware of the left-lateral faults or the significance of the relationship between the two different fault sets and their role in the evolution of the fault network pattern. Many strike-slip fault valleys are intruded by igneous dikes (Fig. 11), and some have small elongated lakes (Fig. 7A).

Both sets of strike-slip faults are found in the coarse-grained units, and to a lesser degree in sandy intervals in the fine-grained units. The average orientation of the fault sets are 058° (NE–SW) and 087° (E–W), for the right-lateral and left-lateral sets, respectively. Some variation in the orientation of the left-lateral set

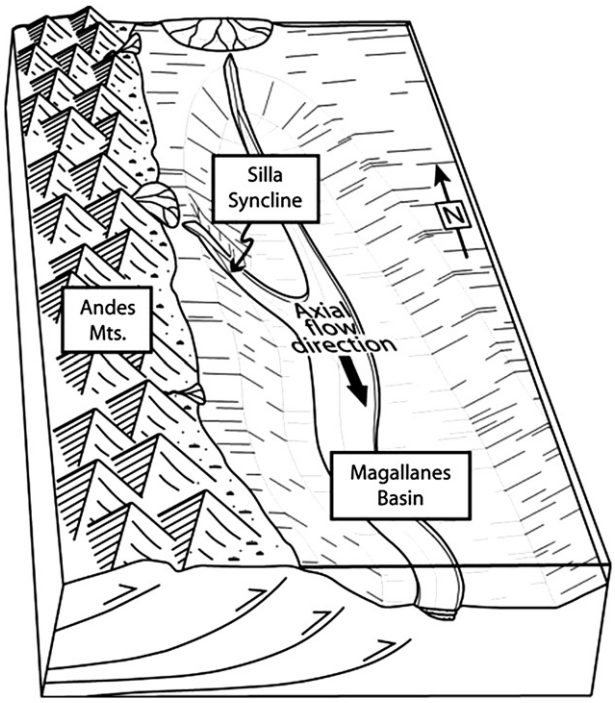

Fig. 6. Schematic diagram of the depositional setting the Late Cretaceous showing the Silla syncline as a feeder channel to the larger Magallanes Basin. After Hubbard (2006).

from generally E–W, to NW–SE occurs in the western part of the study area. There are several differences between the two fault sets, including length, offset, and frequency. In general fault length and displacement are larger for the right-lateral set, with an average segment length of approximately 450 m and a maximum slip of approximately 40 m. For the left-lateral set, the average segment length is approximately 330 m and the maximum slip is approximately 8 m. Fig. 12 presents histograms of the measured fault length and offset for the right- and left-lateral faults. The frequency of right-lateral faults is greater than that of the left-lateral faults, with a ratio of approximately 3:1 (Fig. 7A).

The width of the strike-slip fault valleys is likely an expression of the damage zone, or zone of increased fracturing around the fault, which generally increases with slip along the fault (Scholz, 2002; Flodin and Aydin, 2004; Myers and Aydin, 2004; de Joussineau and Aydin, 2007). To illustrate the presence and characteristic of the damage zone, we measured fracture distribution at the shoulders of a fault valley with approximately 5 m right-lateral offset. Fig. 13 shows the relations between fracture frequency and orientation within a conglomerate unit on both sides of the fault valley. The distribution of the NW SE and E W oriented fractures does not appear to be significantly influenced by the fault location, but the NE SW oriented fracture frequency increases when approaching the fault, showing the change from the background fracture frequency to that of the increased fracturing near the fault. This orientation corresponds to the splay orientation associated with the right-lateral shearing of the fault. The increase in the number of fractures enhances weathering and erosion. As a result, prominent valleys in the study area are most often the locations of somewhat larger (greater than 10 m offset) right-lateral strike-slip faults although most strike-slip faults will have similar morphological expressions.

4.1.3. Fractures

Most outcrops contain three or more fracture sets (Fig. 14). The most prominent is oriented roughly E–W, or perpendicular to the bedding strike. A less common set is a strike-parallel set in an approximate N–S orientation, which is characterized by discontinuous wavy traces on bedding surfaces. A set oriented NE–SW, oblique to the E–W set is also seen. In addition, another set oblique to the E–W set but in a NW–SE direction occurs in some places. These oblique sets commonly abut the prominent E–W set and therefore are younger and indicate a complicated pattern of shearing across the E–W set.

Fracture occurrence varies with lithology and bed thickness. Generally, sandy intervals in the fine-grained, thinly bedded units display higher fracture frequency than the massive coarse-grained units (Figs. 5 and 14). This is in part due to the effect of bed thickness on joint spacing (Pollard and Aydin, 1988). Generally, coarse sandstone layers have fewer but more continuous fractures (Fig. 14A), whereas less coarse sandstone layers have an increased number of fractures with narrower spacing nearly proportional to the layer thickness (Fig. 14B). Furthermore, fractures in sandstone layers do not propagate into any adjacent mudstone layers. This type of fracture truncation at fine-grained layer interfaces results in discontinuous fractures confined in coarser-grained layers (Helgeson and Aydin, 1991), implying that the greater the mud ratio, the more discontinuous the fractures.

4.1.4. Intrusive structures

The Magallanes Basin experienced several episodes of intrusive activity in the mid-Miocene (Altenberger et al., 2003). The distinctive Paine massif is the most prominent intrusion, and is located directly to the north (Fig. 2) of the study area. Within the study area, mafic dikes oriented parallel to strike-slip faults are most common (Fig. 11), although a few sills oblique to the strike-slip faults and/or at low angle to bedding also occur. In the well-developed strike-slip fault valleys, the dikes are present along the valley walls. While the majority of intrusions are dikes or sills, some are intrusive plugs located at the faults' stepovers (Aydin et al., 1990). A characteristic feature of many dikes is a left- or right-stepping en echelon pattern, which is likely a product of dike emplacement process (Delaney and Pollard, 1981; Baer, 1991).

4.2. Temporal relationships based on field observations

Cross-cutting relationships indicate the following temporal relationships between the previously discussed elements. The E–W oriented fracture set likely began to form early in the deformational history of the area. These fractures are consistent with the orogen perpendicular compression responsible for the folding and E–W contraction. However, new fracture formation and development evidently continued throughout each of the following deformation phases as either the earlier fractures or the principal stresses were rotated from the principal stress planes and consequently were sheared. Besides the E–W oriented fractures, folds and thrust faults are the oldest structural elements. This phase of deformation localized the accumulation of coarse-grained sandstone and conglomerate channel deposits, which were then cut by strike-slip faults. Strike-slip faulting initiated after thrust faulting and folding began, but was active contemporaneous with folding and thrust faulting. The intrusive activity began after strike-slip fault formation, because many of the dikes are intruded into strike-slip fault zones. Fig. 15 shows a dike intruded into a left-lateral fault, and in turn, offset of the dike by a bedding plane fault related to the flexural slip mechanism associated with the tightening of the Silla Syncline. This provides constraints for the sequence of deformation at this location: Strike-slip fault development, dike intrusion along the fault, followed by fold growth. In other cases, dikes and

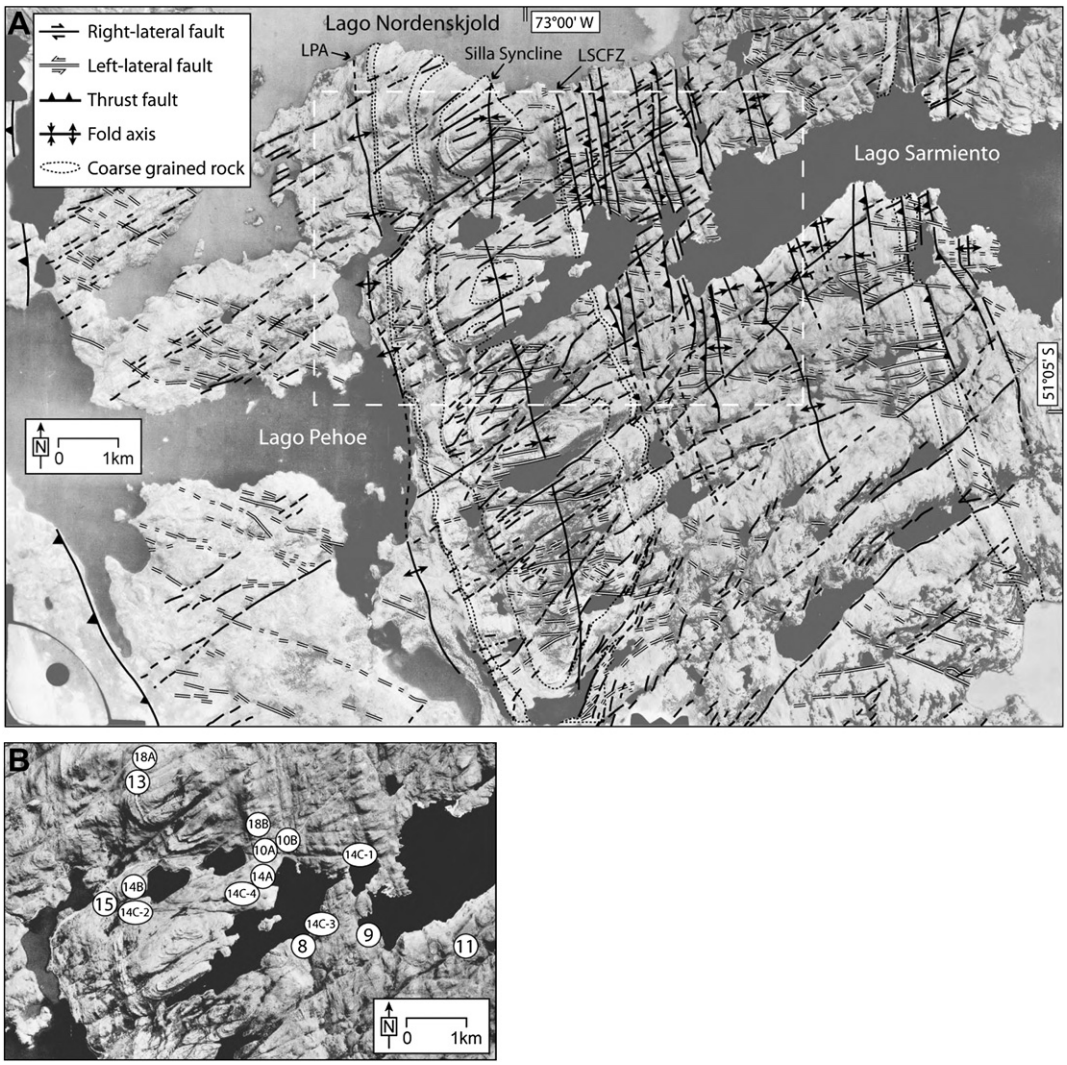

Fig. 7. (A) Structural map of the study area showing major folds, thrust faults, and strike-slip faults. LPA, Lago Pehoe Anticline; LSCFZ, Lago Sarmiento Chico Fault Zone. Coarse-grained rock locations taken from Crane (2004). Dashed box is the location for (B), location map for figures within the study area.

sills oriented oblique to strike-slip fault zones are offset across the fault (Fig. 11). These cross-cutting relationships indicate that the thrust-cored folding and strike-slip faulting continued after the intrusions were emplaced.

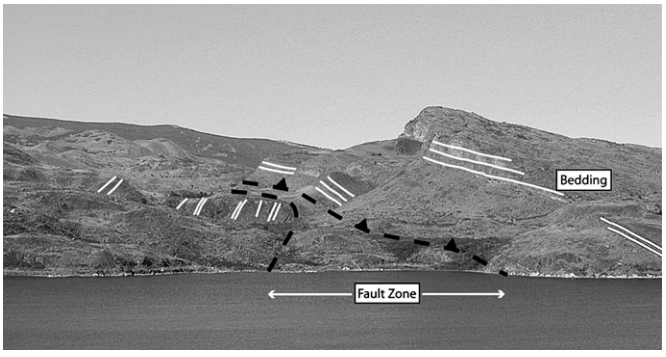

Fig. 8. View to the south along the Lago Sarmiento Chico Fault Zone, with the eastern limb of the Silla Syncline visible on the right of the photograph. The width of the fault zone is approximately 250 m at lake level.

5. Implications and discussion

Based on the field data and temporal framework presented above, we interpret the relationships between structural features (fractures, strike-slip faults, and thrust faults) and between structural features and the location and attributes of coarse-grained channel deposits.

5.1. Strike-slip fault formation from fractures

The strike-slip faults developed from the pre-existing fractures. To clarify this mechanism, we examined the character of the different fractures and strike-slip fault sets from the outcrop scale (Fig. 14) to the aerial photograph scale (Fig. 7A). The E–W fractures have an opening mode surface morphology and an orientation roughly parallel to the direction of regional compression. This is consistent with the concept that these fractures initially formed in opening mode as joints (Pollard and Aydin, 1988) during the initial stage of folding or during the fold development (Moretti et al., 2007; Guiton et al., 2003). Many of the cross fractures have splay fractures, also known as tail cracks, horsetail fractures, or kink cracks, which indicate that the cross fractures were later sheared. Consequently, based on field observations of the strike-slip faults at

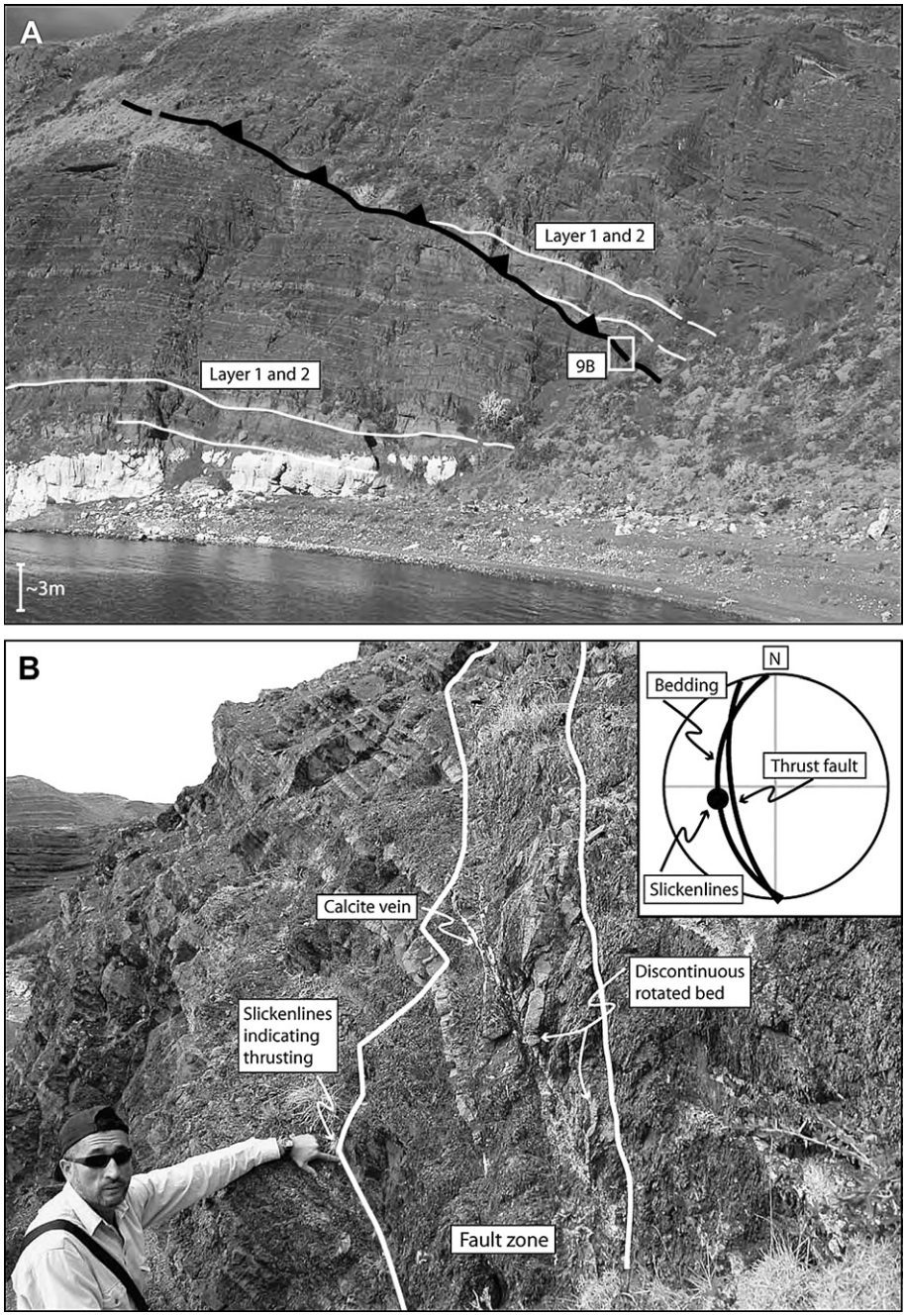

Fig. 9. (A) Thrust fault with approximately 30 m offset. View is to the south-southwest with the plane of the fault is dipping into the page. (B) Detail of the fault zone in (A), showing typical fault zone features such as calcite veins and discontinuous bedding.

various scales in the study area, it appears that a hierarchical, sheared joint-based mechanism of faulting (Myers and Aydin, 2004) has taken place in the area and has produced the apparent conjugate fault pattern (Flodin and Aydin, 2004; Florez-Nino et al., 2005) as discussed below.

Our field observations indicate that faults developed from shearing across E–W joints (Fig. 14) which are more pervasive among the fracture network. Shearing across these E–W joints was the result of either a material rotation, or a rotation of the remote stresses as shown in Fig. 16. Because the initial E–W joints were short and closely spaced (Fig. 16A), fault growth required linkage of adjacent sheared joints (Fig. 16B). The configuration that promotes the most efficient linkage is that of neighboring joints with right sense of stepping to form right-lateral faults and left sense of stepping to form left-lateral faults (Fig. 16C). Thus faults are often oriented slightly oblique to the initial joint orientation. Because of this mechanism of fracture linkage, the fault damage zones become longer and wider as linkage among sheared fractures at greater distance occurs.

For the larger strike-slip fault network, the mechanism for the formation of the apparent conjugate fault system is more complex (Fig. 16D). Here, the second generation fractures are also sheared but in a sense opposite to the shearing across the initial fault. As a result, the network is composed of two fault sets with complementary slip senses and with an intersection angle dictated by the angle that a splay fracture makes with the initial sheared joint

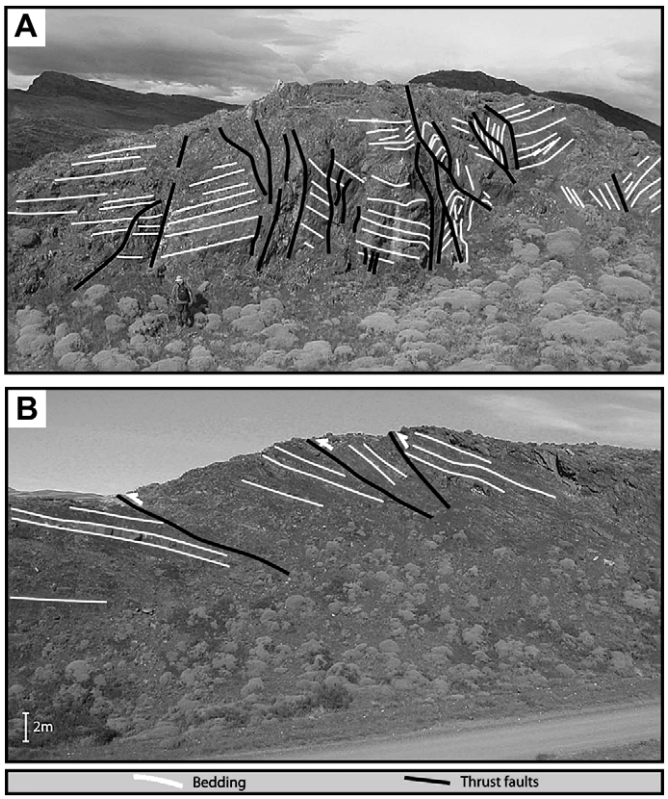

Fig. 10. (A) Complex fold and fault coupling geometries, and (B) low angle wedge shaped faults. The view direction for both (A) and (B) is to the south.

(Davatzes and Aydin, 2003; Flodin and Aydin, 2004; de Joussineau et al., 2007), as opposed to an intersection angle based on the friction angle as predicted by the Coulomb failure criterion (Anderson, 1951).

As discussed previously there are differences in the segment length, slip magnitude, and frequency of the two faults sets. It appears that the right-lateral set is dominant, as it has a larger segment length, greater maximum fault slip, and is more prevalent throughout the study area. The cause of this is likely related to the driving force responsible for the deformation, such that the right-lateral faults make a smaller angle to the greatest compression (Fig. 16C and D) and are the preferential locations for larger slip.

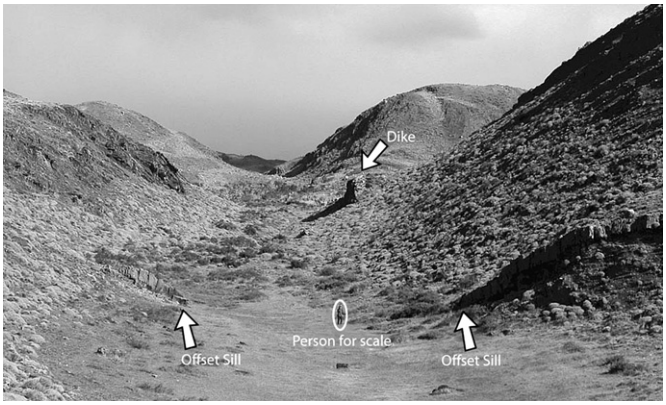

Fig. 11. View looking southwest along a strike-slip fault valley with 13 m right-lateral offset, with a dike intrusion along the valley, and a sill oblique to the valley.

5.2. Strike-slip and thrust fault interplay

Based on field relationships, it is likely that strike-slip faulting and thrust faulting were active simultaneously (Fig. 15), although thrust faulting and folding appear to have initiated first (Figs. 7A and 17). Having both types of faults active at the same time is consistent with the predominant E–W compression that is the mutual driving force, as well as with mechanical models of folded layers. Guiton et al. (2003) used mechanical models to show that during the folding of a layer, the stress distribution is such that there is the potential for both strike-slip and reverse faults to be active at the same time, in orientations consistent with those reported in this study.

The interplay of strike-slip and thrust faults also raises an issue in terms of the Anderson theory of faulting. For thrust faults, the minimum principal stress is vertical, whereas for strike-slip faults the intermediate principal stress is vertical. Therefore according to the Anderson theory of faulting these principal stresses would have to interchange periodically for the co-development of the thrust and strike-slip faults. This possible interchange would imply that the minimum and intermediate principal stresses were similar in magnitude, and that small perturbations were capable of a re-organization of the principal stresses in certain domains. However, our study shows that other factors, such as lithology and contrasting mechanical properties of the depositional sequences are also important in portioning the thrust and strike-slip faulting domains. The details of the interplay between the depositional and deformational processes will be further elaborated in the following section.

5.3. Depositional architecture

Previous studies have demonstrated a link between structural elements and depositional processes at other locations, such as the San Joaquin Basin in California (Reid, 1990; Link and Hall, 1990), the South Spanish Pyrenees (Grecula et al., 2003), and South Africa (Pickering and Corregidor, 2005). However, in the Magallanes Basin, while previous studies have shown the Silla Syncline to be a feeder channel into the basin likely related to tectonic processes (Wilson, 1991; Crane, 2004; Hubbard, 2006), the way in which structural deformation influenced the depositional architecture was not explicitly identified.

Considering the distribution of the sediments across the Silla Syncline, it is interesting that coarse-grained sediments are confined to the syncline between the bounding structures, the LPA on the west side and the LSCFZ on the east side. Fig. 17 is a cross section illustrating the bounding structures in relation to the coarse-grained deposits. Because of the asymmetrical nature of the LPA fold structure, we infer that the fold is associated with a west-dipping thrust fault at depth. Also, the coarse-grained deposits do not cover the entire width of the syncline, and their channels are discontinuous with shifting locations both laterally and vertically (Crane, 2004).

Based on the framework described above, we interpret the confinement of the conglomerates and coarse-grained sandstones to be caused by the two bounding structures, the LPA and LSCFZ, and propose that these structures had initiated prior to the arrival of the channel deposits. As these bounding structures accommodated more strain, the area between them evolved into a broad flat syncline that formed a trough in which channels were localized. Therefore, the mechanism of syncline formation was bending at predetermined boundaries. This resulted in a fold geometry with a long and flat center and localized higher curvature at the shoulders, close to the boundary structures.

From this perspective, the depositional history of the coarse-grained sandstone and conglomerate within the core of the

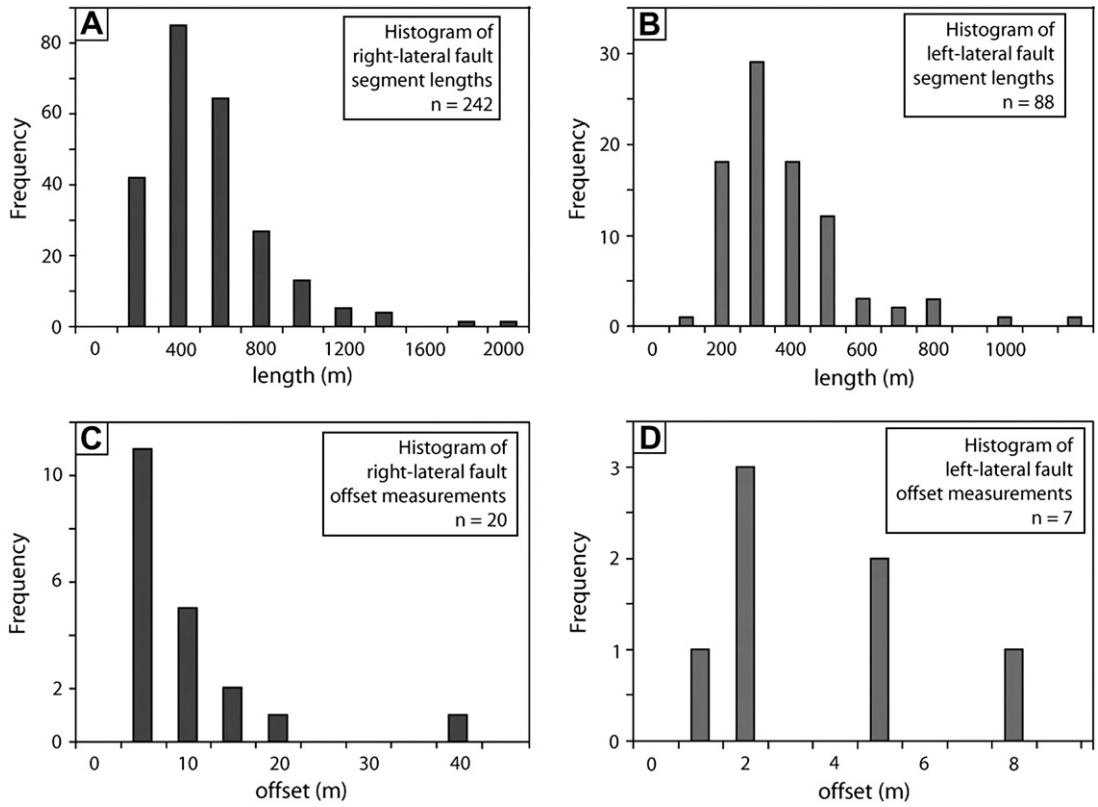

Fig. 12. (A) Histogram for right-lateral fault segment length. (B) Histogram for left-lateral fault segment length. (C) Histogram for right-lateral fault offset measurements. (D) Histogram for left-lateral fault offset measurements.

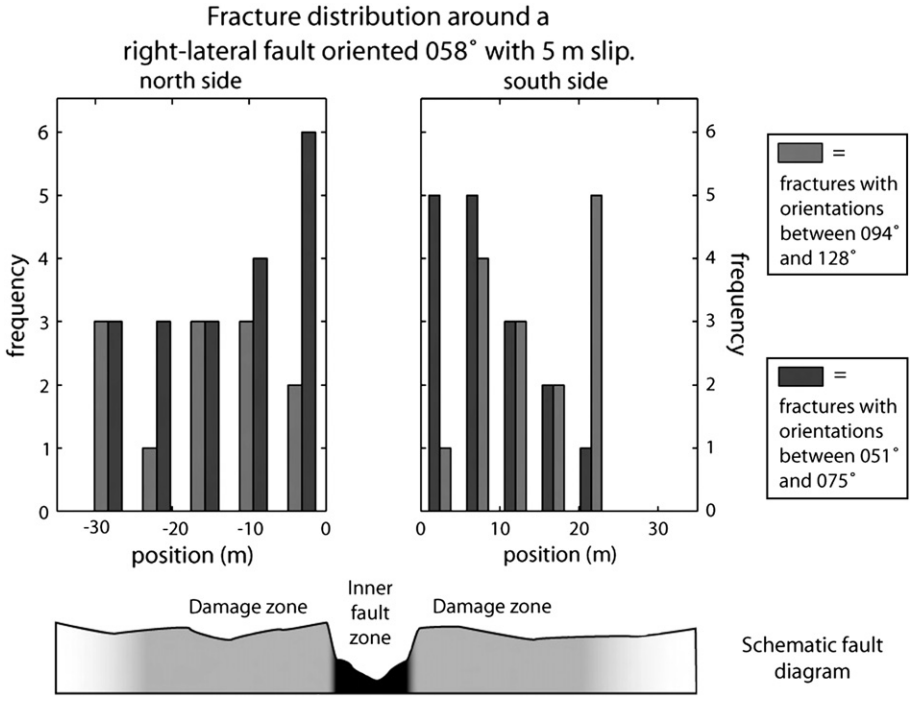

Fig. 13. Fracture orientation and density from a scanline across a right-lateral fault, showing an increase in NE–SW oriented fractures moving towards the fault zone.

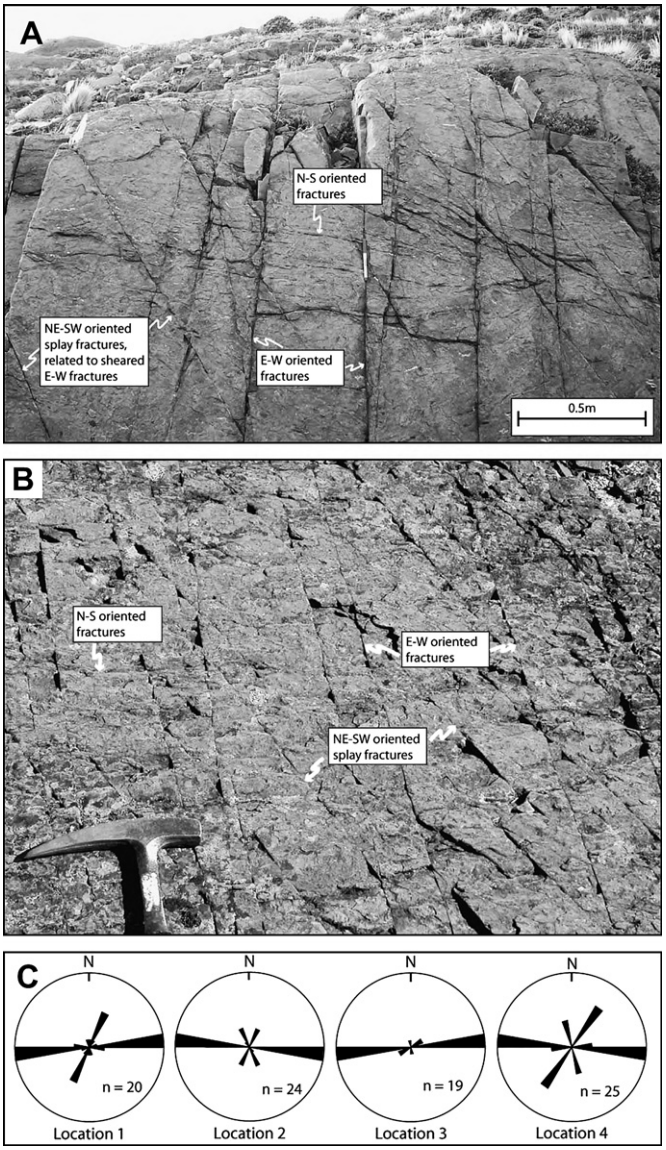

Fig. 14. (A) View to the east, showing typical fracture sets of the study area in a coarse sandstone outcrop. (B) View to the west, showing typical fracture sets in a fine grained outcrop. (C) Rose diagrams of fracture measurements in the study area, outcrop locations are shown in Fig. 7B.

syncline should be related to the growth history and evolution of the boundary structures. Thus, it is reasonable to interpret the depositional architecture of the channel margins around the perimeter of the syncline in terms of the underlying boundary structures. These depositional structures include abrupt changes and truncations in bed orientations, and onlapping relationships as shown in Fig. 18, with (A) showing the western limb and (B) the eastern limb. At the base of the coarse-grained units, the variation in dip orientation, bedding juxtapositions, and onlap behavior indicates ongoing deformation during the deposition of younger units. While some discordant contacts at the base of coarse-grained units could be interpreted as purely erosional or represent depositional dip on a levee surface, the change of dip angle from older to younger layers and the proximity of these changes to the underlying faults and related growth folds are conspicuous. Considering the distribution of the coarse-grained deposits and that they abut the boundary structures, we propose that the location, orientation, and depositional timing of the channel deposits are intimately related to the underlying bounding structures.

If the formation of the boundary structures, the LPA and LSCFZ, began before the first appearance of the coarse-grained units, the spacing of these two features would be determined by factors other than the distribution of the coarse-grained sandstones and conglomerates. From Figs. 2 and 19 there appears to be a regional spacing to large-scale folds and thrust faults, as well as the locations of coarse-grained deposits. Generally, the spacing between these large features ranges from 4 to 10 km, which is in the same order as the 4 km spacing between the LPA and LSCFZ. This spacing is likely to be the result of the fold and thrust belt spacing in the underlying units.

In addition to the focused deposition in the structurally controlled trough, channel migration could be caused by a sequential deformation in either limb of the newly forming Silla Syncline in response to a particular thrust episode and related growth structure. In this case, subsidence associated with intermittent slip on the bounding fault system could result in migrating channel locations.

The change in sediment size from fine-grained to coarse-grained has also been attributed to tectonic activity (Crane, 2004). After fine-grained deposition, tectonic uplift of the Andes to the west likely initiated the deposition of the coarse sandstones and conglomerates found in the Silla Syncline (Crane, 2004; Coleman, 2000). We propose that the eastward propagation of the Andean contractional deformation in the form of thrust cored folds, in addition to increasing contraction and uplift of the Andean highlands to the west, created an environment for the deposition of the coarse-grained sandstones and conglomerates to the east in the Silla Syncline and its surrounding area.

6. Conclusions

The structural geology of the Silla Syncline and surrounding area sheds light on a number of deformational and depositional features including the patterns of, and interrelationships among, strike-slip faults and thrust faults, deposition of coarse-grained channel deposits, and pathways for igneous intrusions in a foreland basin. Specifically, the locations of coarse-grained channel deposits within the syncline were controlled by the first order thrust faults and related folds that initiated prior to the coarse sediment deposition. These folds created a fold geometry with a broad flat center and higher curvature at the tight limbs, which is different than that expected from buckling related folding. It appears that the strike-slip fault network developed by a sheared joint-based mechanism is responsible for the apparent conjugate fault sets composed of the right- and left-lateral faults. During the deformational history of the area, the strike-slip faults and thrust faults and related folds were active contemporaneously. This co-activity continued to at least the mid-Miocene.

Based on our field data, we propose a conceptual model for the development of the structural and depositional elements, with a schematic structural diagram shown in Fig. 20. Regional compression in the Late Cretaceous resulted in the formation of a foreland fold and thrust belt in the Magallanes Basin. At the local scale, this compression and the resulting thrust faults and folds helped to control the location of coarse-grained sandstones and conglomerates of the Silla Syncline. Folding and faulting continued, further involving kilometer scale folds like the Silla Syncline in coarse-grained units, and many smaller folds in fine-grained units.

A possible regional stress rotation or material rotation could mark the onset of strike-slip faulting in the area. The formation

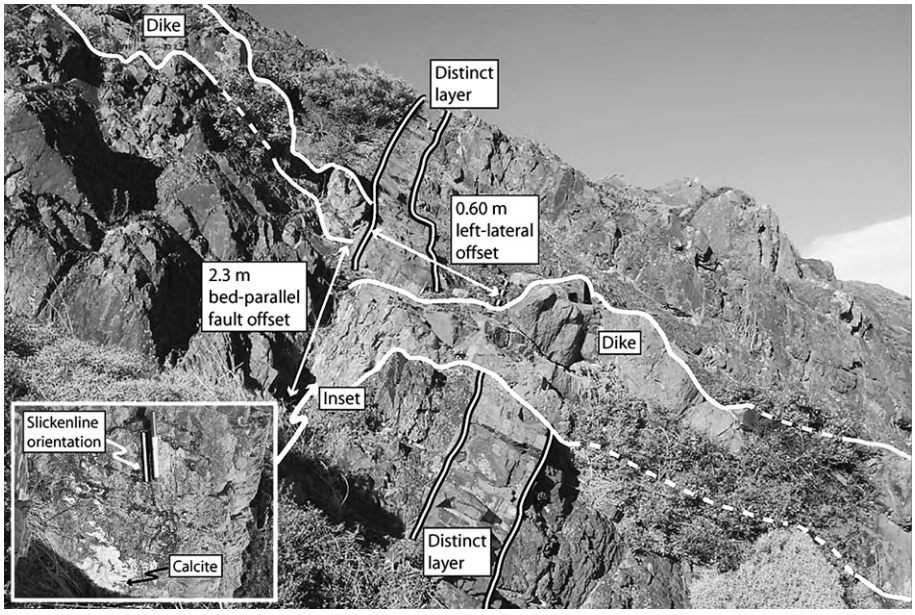

Fig. 15. View to the south of an intrusive dike along a left-lateral strike-slip fault with 0.60 m offset. Dike has also been cut by a bed parallel fault with 2.3 m offset. Inset shows the bed parallel fault surface on the dike.

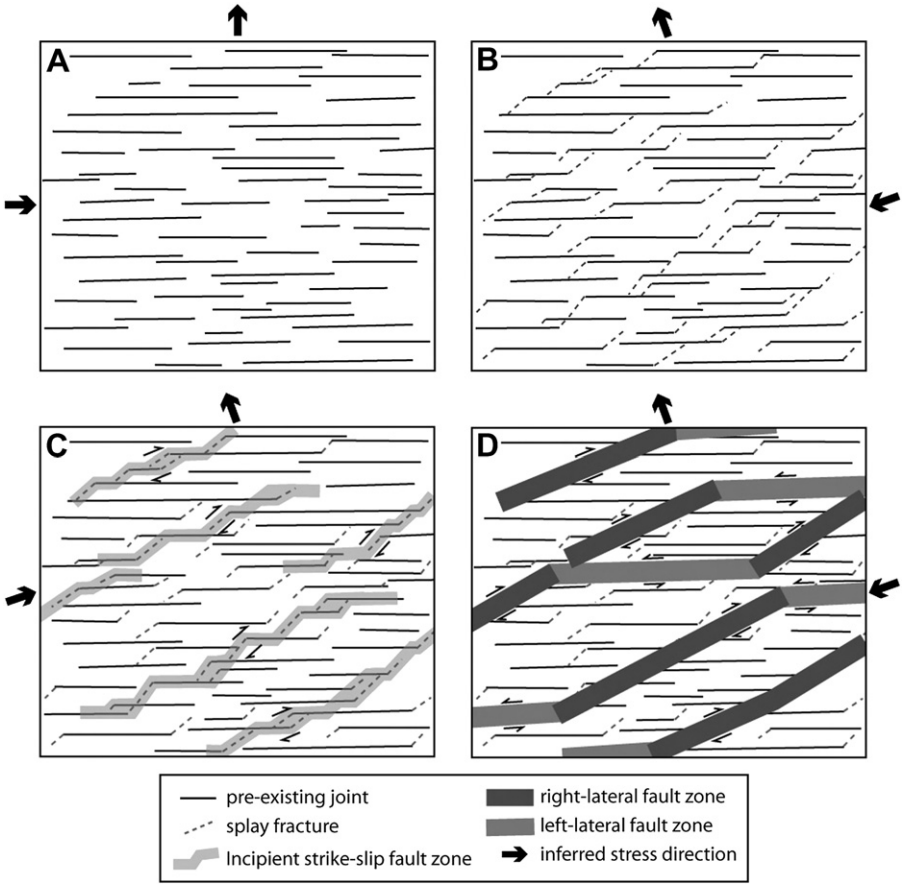

Fig. 16. (A) Pre-existing joint configuration. (B) Left-lateral shearing along joints, producing splay fractures. (C) Faults developing by linkage of neighboring segments. (D) Right-lateral faults forming through sheared cross joints and splay fractures. Left-lateral faults form along splay fractures associated with right-lateral faults.

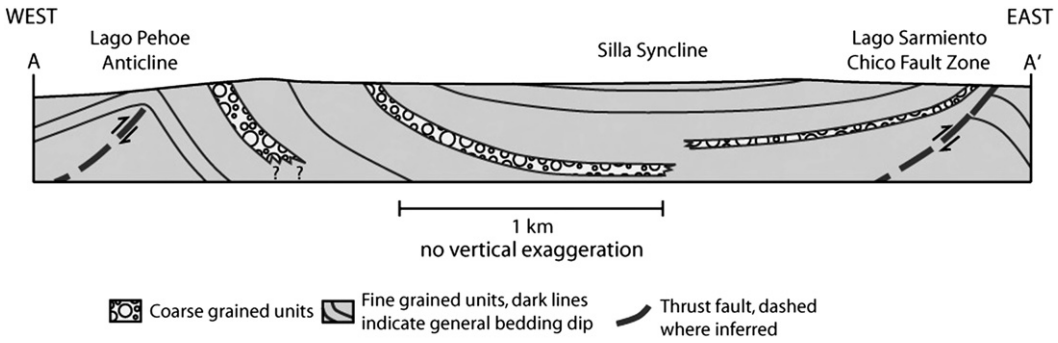

Fig. 17. Cross section across the Silla syncline, showing coarse-grained deposits and their relations to the bounding fault anticline (west) and complex thrust fault zone (east). See Fig. 2 for cross section location.

of these faults utilized the pre-existing cross-fracture system primarily in the coarser and stiffer units within the Silla Syncline to form in a hierarchical manner, with right-lateral faults forming first and left-lateral faults developing from splays off of the right-lateral set. Continued slip along the right-lateral set resulted in the dominance of that set as observed in the study area. Thrust faults were still active at this time and were primarily confined within the fine-grained units. These thrust faults and folds along with the strike-slip faults accommodated E–W contraction. In the Cenozoic, the deformation continued intermittently with the igneous activity beyond the mid-Miocene as many intrusions are cross cut by flexural slip faults, as

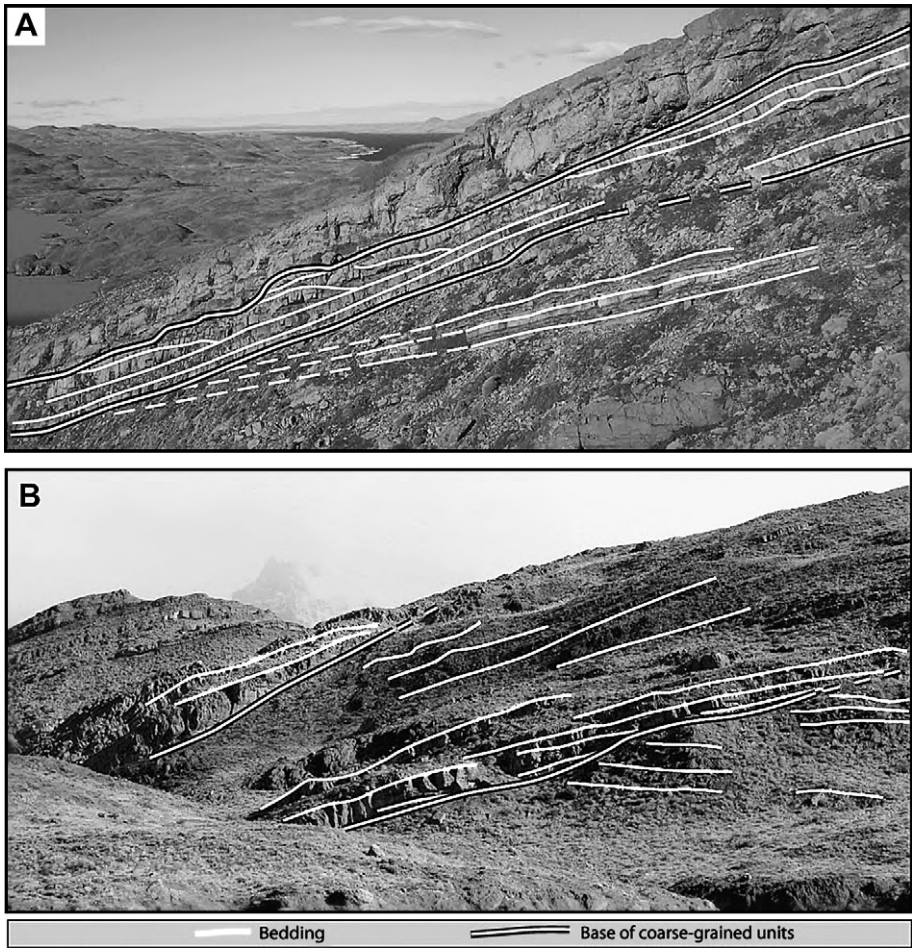

Fig. 18. (A) Angular relationship of sediment layers underlying a conglomerate near Lago Nordenskjold. Location is on the western limb of the Silla syncline, above the Lago Pehoe anticline, looking to the east. (B) Angular relationships between sedimentary layers at the base of coarse-grained units. Location is on the eastern limb of the Silla syncline, above the Lago Sarmiento Chico fault zone, looking west-northwest.

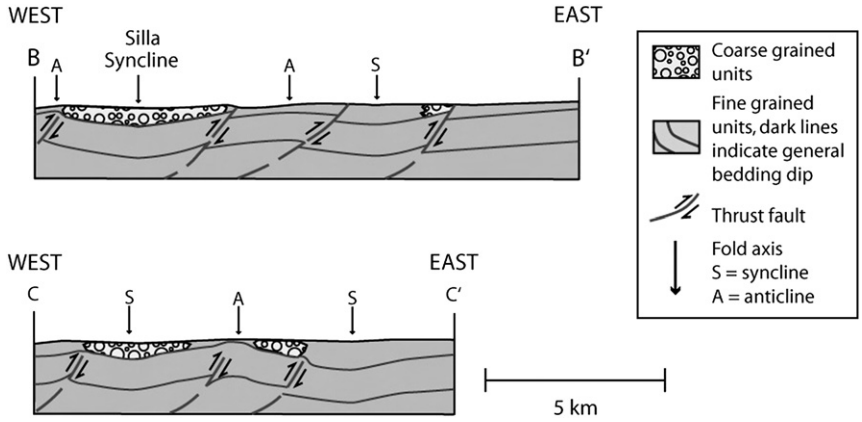

Fig. 19. Schematic cross section across the Cerro Toro Formation (see Fig. 2 for cross section locations), showing the periodicity of coarse units and fold axes.

well as the strike-slip faults. However, many of the dikes intruded into the strike-slip faults providing a variety of cross-cutting relationships.

In summary, the field data and the conceptual models provided in this paper should be helpful to visualize the types of structures, their temporal and spatial interrelationships, and their distributions with respect to various lithological units making up the deep-water deposits within the Magallanes foreland basin. The interplay between (1) the distribution and depositional architecture of the coarse-grained deposits at the channel margins and the thrust faults and related anticlines, (2) the thrust faults and the contemporaneous strike-slip faults, and (3) strike-slip faults and dike intrusions are intriguing and require future multidisciplinary research efforts for a more complete understanding of these relationships.

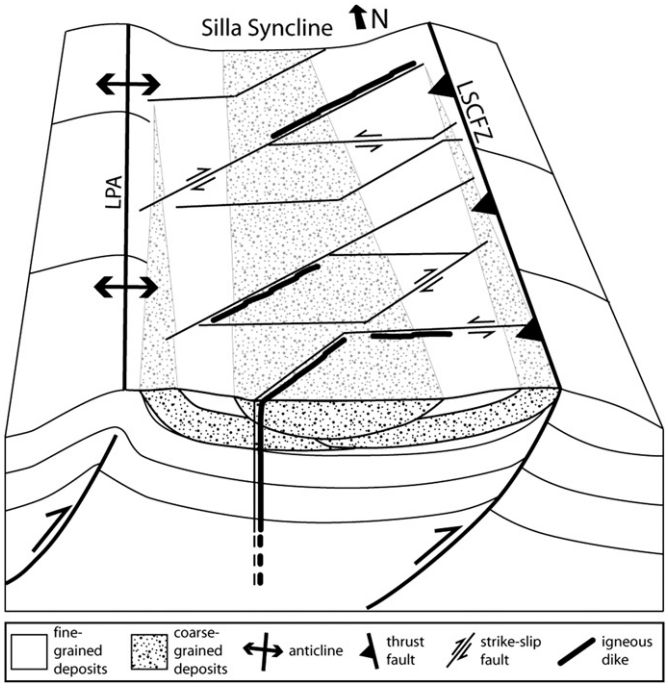

Fig. 20. Schematic diagram of the Silla syncline showing thrust faults, folds, strike-slip faults, igneous dikes, and the location of coarse-grained depositional channels.

Acknowledgements

This work was supported by the Stanford Rock Fracture Project. The base aerial photograph of the study area was obtained from Steve Graham who had received the original from Terry Wilson. We would like to thank Ronald Bruhn for his review of an early version of this manuscript. Steve Graham and Ghislain de Joussineau also provided early reviews of the manuscript, and Donald Lowe gave his insights on the architecture of the channel deposits along the Silla Syncline. We thank Will Crane, Andrea Fildani, and Stephen Hubbard for sharing their research results with us. We also thank the administration in the Parque Nacional Torres del Paine and the Corporación Nacional Forestal de Chile (CONAF) for their permission to undertake this study.

References

Altenberger, U., Oberhansli, R., Putlitz, B., Wemmer, K., 2003. Tectonic controls and Cenozoic magmatism at the Torres del Paine, southern Andes (Chile, 51°10'S). Revista Geológica de Chile 30 (1), 65–81.

Anderson, E.M., 1951. The Dynamics of Faulting. Oliver and Boyd, White Plains, NY.

Aydin, A., Schultz, R.A., Campagna, D., 1990. Fault-normal dilation in pull-apart basins: implications for the relationship between strike-slip faults and volcanic activity. Annales Tectonicae 4 (2), 45–52.

Baer, G., 1991. Mechanisms of dike propagation in layered rocks and in massive, porous sedimentary rocks. Journal of Geophysical Research 96 (B7), 11911–11929.

Biddle, K.T., Uliana, M.A., Mitchum Jr., R.M., Fitzgerald, M.G., Wright, R.C., 1986. The stratigraphic and structural evolution of the central and eastern Magallanes Basin, southern South America. In: Allen, P.A., Homewood, P. (Eds.), Foreland Basins. International Association of Sedimentologists, vol. 8. Special Publication, pp. 41–63.

Bruhn, R.L., Stern, C.R., de Wit, M.J., 1978. Field and geochemical data bearing on the development of a Mesozoic volcano-tectonic rift zone and back-arc basin in southernmost South America. Earth and Planetary Science Letters 41, 32–46.

Coleman, J.L., 2000. Reassessment of the Cerro Toro (Chile) sandstones in view of channel-levee-overbank reservoir continuity issues, in: Weimer, (Ed.), Deep-water Reservoirs of the World: Gulf Coast Section. 20th Annual Research Conference, Society of Economic Paleontologist and Mineralogists, pp. 252–258.

Crane, W.H., 2004. Depositional history of the Upper Cretaceous Cerro Toro Formation, Silla Syncline, Magallanes Basin, Chile. PhD thesis, Stanford University, Stanford, CA, 275 pp.

Dalziel, I.W.D., 1981. Back-arc extension in the Southern Andes: a review and critical reappraisal. Royal Society of London Philosophical Transactions, Series A 300, 319–335.

Dalziel, I.W.D., de Wit, M.J., Palmer, K.F., 1974. Fossil marginal basin in the southern Andes. Nature 250, 291–294.

Davatzes, N.C., Aydin, A., 2003. The formation of conjugate normal fault system in folded sandstone by sequential jointing and shearing, Waterpocket monocline, Utah. Journal of Geophysical Research 108 (B10), 2478.

de Joussineau, G., Aydin, A., 2007. The evolution of the damage zone with fault growth in sandstone and its multiscale characteristics. Journal of Geophysical Research 112, B12401, doi:10.1029/2006jb004711.

de Joussineau, G., Mutlu, O., Aydin, A., Pollard, D., 2007. Characterization of fault-splay relationships: field survey and mechanical modeling. Journal of Structural Geology 29, 1831–1842, doi:10.1016/j.jsg.2007.08.006.

Delaney, P.T., Pollard, D.D., 1981. Deformation of host rocks and flow of magma during growth of minette dikes and breccia-bearing intrusions near Ship Rock, New Mexico. US Geological Survey Professional Paper, No. 1202, pp. 1–61.

Fildani, A., Cope, T.D., Graham, S.A., Wooden, J.L., 2003. Initiation of the Magallanes foreland basin: timing of the southernmost Patagonian Andes orogeny revised by detrital zircon provenance analysis. Geology 31 (12), 1081–1084.

Fildani, A., Hessler, A.M., 2005. Stratigraphic record across a retroarc basin inversion: Rocas Verdes-Magallanes Basin, Patagonian Andes, Chile. Geological Society of America Bulletin 117 (11/12), 1596–1614.

Flodin, E.A., Aydin, A., 2004. Evolution of a strike-slip fault network, Valley of Fire State Park, southern Nevada. Geological Society of America Bulletin 116 (1/2), 42–59.

Florez-Nino, J.M., Aydin, A., Mavko, G., Antonellini, M., Ayaviri, A., 2005. Fault and fracture systems in a fold and thrust belt: an example from Bolivia. Bulletin of the American Association of Petroleum Geologists 89 (4), 471–493.

Grecula, M., Flint, S., Potts, G., Wickens, D., Johnson, S., 2003. Partial ponding of turbidite systems in a basin with subtle growth-fold topography; Laingsburg-Karoo, South Africa. Journal of Sedimentary Research 73 (4), 603–620.

Guiton, M.L.E., Leroy, Y.M., Sassi, W., 2003. Activation of diffuse discontinuities and folding of sedimentary layers. Journal of Geophysical Research 108 (B4), 2183.

Gust, D.A., Biddle, K.T., Phelps, D.W., Uliana, M.A., 1985. Associate Middle to Late Jurassic volcanism and extension southern South America. Tectonophysics 116, 223–253.

Helgeson, D.E., Aydin, A., 1991. Characteristics of joint propagation across layer interfaces in sedimentary rocks. Journal of Structural Geology 13 (8), 897–991.

Hubbard, S.M., 2006. Deep-sea foreland basin axial channels and associated sediment gravity flow deposits, Oligocene Molasse basin, Upper Austria, and Cretaceous Magallanes Basin, Chile. PhD thesis, Stanford University, Stanford, CA, 217 pp.

Katz, H.R., 1962. Fracture patterns and structural history in the sub-Andean belt of southernmost Chile. Journal of Geology 70 (6), 595–603.

Katz, H.R., 1963. Revision of Cretaceous stratigraphy in Patagonian cordillera of Ultima Esperanza, Magallanes Province, Chile. Bulletin of the American Association of Petroleum Geologists 47 (3), 506–524.

Kraemer, P.E., 2003. Orogenic shortening and the origin of the Patagonian orocline (56°S. lat). Journal of South American Earth Sciences 15, 731–748.

Link, M.H., Hall, B.R., 1990. Architecture and sedimentology of the Miocene Moco T and Webster turbidite reservoirs, Midway-Sunset Field, California. In: Kuespert, J.G., Reid, S.A. (Eds.), Structure, Stratigraphy and Hydrocarbon Occurrences of the San Joaquin Basin, vol. 64. Field Trip Guidebook – Pacific Section. Society of Economic Paleontologists and Mineralogists, California, pp. 115–129.

Moretti, I., Delos, V., Letouzey, J., Otero, A., Calvo, J.C., 2007. The use of surface restoration in foothills exploration: theory and application to the sub-Andean zone of Bolivia. In: Lacombe, O., Lavé, J., Roure, F., Vergès, J. (Eds.), Thrust Belts and Foreland Basins; from Fold Kinematics to Hydrocarbon Systems. Frontiers in Earth Sciences, pp. 149–162.

Myers, R., Aydin, A., 2004. The evolution of faults formed by shearing across joint zones in sandstone. Journal of Structural Geology 26, 947–966.

Pickering, K.T., Corregidor, J., 2005. Mass transport complexes and tectonic control on confined basin-floor submarine fans, middle Eocene, south Spanish Pyrenees. In: Hodgson, D.M., Flint, S.S. (Eds.), Submarine Slope Systems; Processes and Products. Geological Society, vol. 244. Special Publications, London, pp. 51–74.

Pollard, D.D., Aydin, A., 1988. Progress in understanding jointing over the past century. Geological Society of America Bulletin 100, 1181–1204.

Reid, S.A., 1990. Trapping characteristics of upper Miocene turbidite deposits, Elk Hills Field, Kern County, California. In: Kuespert, J.G., Reid, S.A. (Eds.), Structure, Stratigraphy and Hydrocarbon Occurrences of the San Joaquin Basin, vol. 64. Field Trip Guidebook – Pacific Section. Society of Economic Paleontologists and Mineralogists, California, pp. 141–156.

Scholz, C.H., 2002. The Mechanics of Earthquakes and Faulting. Cambridge University Press, Cambridge, 471 pp.

Wilson, T.J., 1983. Stratigraphic and structural evolution of the Ultima Esperanza foreland fold-thrust belt, Patagonian Andes, Southern Chile. PhD dissertation, Columbia University, New York, 360 pp.

Wilson, T.J., 1991. Transition from back-arc to foreland basin development in the southernmost Andes: stratigraphic record from the Ultima Esperanza District, Chile. Geological Society of America Bulletin 103, 98–111.

Winslow, M.A., 1981. Mechanisms for basement shortening in the Andean foreland fold belt of southern South America. In: McClay, K.R., Price, N.J. (Eds.), Thrust and Nappe Tectonics. Geological Society, vol. 9. Special Publications, London, pp. 513–529.